# Catalytic Hydrogenation of a Manganese(V) Nitride to Ammonia

Sangmin Kim, Hongyu Zhong, Yoonsu Park, Florian Loose, and Paul J. Chirik*

Department of Chemistry, Frick Laboratory, Princeton University, Princeton, New Jersey 08544, United States

**ABSTRACT:** The catalytic hydrogenation of a metal nitride to produce free ammonia using a rhodium hydride catalyst that promotes $H_2$ activation and hydrogen atom transfer is described. The phenylimine-substituted rhodium complex, ($\eta^5$-$C_5Me_5$)Rh($^{Me}$PhI)H ($^{Me}$PhI = *N*-methyl-1-phenylethan-1-imine) exhibited higher thermal stability compared to the previously reported ($\eta^5$-$C_5Me_5$)Rh(ppy)H (ppy = 2-phenylpyridine). DFT calculations established that the two rhodium complexes have comparable Rh–H bond dissociation free energies of 51.8 kcal mol$^{-1}$ for ($\eta^5$-$C_5Me_5$)Rh($^{Me}$PhI)H and 51.1 kcal mol$^{-1}$ for ($\eta^5$-$C_5Me_5$)Rh(ppy)H. In the presence of 10 mol% of the phenylimine rhodium precatalyst and 4 atm of $H_2$ in THF, the manganese nitride, ($^{tBu}$Salen)Mn≡N underwent hydrogenation to liberate free ammonia with up to 6 total turnovers of $NH_3$ or 18 turnovers of H·. The phenylpyridine analogue proved inactive for ammonia synthesis under identical conditions owing to competing deleterious hydride transfer chemistry. Subsequent studies showed that the use of a non-polar solvent such as benzene suppressed formation of the cationic rhodium product resulting from the hydride transfer and enabled catalytic ammonia synthesis by proton coupled electron transfer.

## INTRODUCTION

The hydrogenation of molecular dinitrogen to ammonia is one of the most important and impactful technological innovations in human history.[1-4] While the Haber-Bosch process relies on high temperature and pressures to combine $N_2$ and $H_2$ to form $NH_3$, it is the most thermodynamically efficient method for ammonia synthesis.[5,6] Exploration of homogeneous catalysts for nitrogen fixation has been motivated by realizing milder reaction conditions and understanding of elementary steps en route to $NH_3$. Several homogeneous ammonia synthesis catalysts are now known and while turnover has been observed at ambient temperature and pressure,[7-18] the reliance on stoichiometric proton and electron sources incurs large chemical overpotentials and poor atom economy.[19]

For homogeneous ammonia synthesis catalysts to operate near thermodynamic potential, dihydrogen ($H_2$) is the optimal stoichiometric reductant.[19-21] The challenge lies in the synthesis of weak N–H bonds as many intermediates in the catalytic cycle range between 30 and 50 kcal mol$^{-1}$, below the driving force for spontaneous $H_2$ formation.[22] Proton coupled electron transfer (PCET) has emerged as a promising strategy for the synthesis of these bonds and examples relevant to ammonia synthesis from metal nitrides include $SmI_2{\cdot}xH_2O$,[23,24] 9,10-dihydroacridine,[25,26] and TEMPO–H.[27] Our group demonstrated this concept using ($\eta^5$-$C_5Me_5$)Rh(ppy)H (**1**) (ppy = 2-phenylpyridine)[28-30] as the hydrogen atom transfer catalyst for the synthesis of ammonia from a titanocene amide complex with $H_2$ as the terminal reductant (Scheme 1a).[20,21] A key feature of the hydrogen transfer catalyst is a M–H bond dissociation free energy (BDFE) higher than 48.6 kcal mol$^{-1}$ ($\Delta G_f°$(H·)) to promote $H_2$ cleavage but also as close to this value as possible to minimize the driving force for N–H bond formation. In the titanocene amide example, the Rh–H BDFE of 52 kcal mol$^{-1}$ in **1** was lower than the incipient N–H bonds of 61 kcal mol$^{-1}$, rendering the overall process spontaneous. Importantly, the rhodium hydride was regenerated by addition of $H_2$ enabling a catalytic reaction.

Hydrogenation of metal nitrides has been of long-standing interest for the synthesis of ammonia following $N_2$ cleavage (Scheme 1b).[31-34] The challenge stems from the low N–H BDFEs of resulting metal imido species and the strong M≡N bond, particularly with those derived from $N_2$ cleavage. Recently, our laboratory reported the application of photodriven proton coupled electron transfer for the synthesis of ammonia from the manganese nitride, ($^{tBu}$Salen)Mn≡N (**MnN**) using a combination of 9,10-dihydroacridine, a ruthenium photocatalyst and a proton source (Scheme 1c).[25,26] The computed, successive N–H BDFEs of 60, 84 and 85 kcal mol$^{-1}$ make this specific metal nitride attractive for ammonia formation. Because of the requirement for 9,10-dihydroacridine as the stoichiometric hydrogen atom source and light as the energy source, this reaction is not ideal for $NH_3$ synthesis in terms of chemical overpotential and overall poor atom economy. Here we describe a thermal, rhodium-catalyzed method for the synthesis of $NH_3$ from **MnN** using $H_2$ as the terminal reductant (Scheme 1c).

**Scheme 1. (a) Catalytic $NH_3$ formation from a titanocene amide complex using $H_2$ as the terminal reductant. (b) Nitride pathway in catalytic $N_2$ reduction via PCET. (c) Catalytic $NH_3$ formation from a manganese nitride using $H_2$ as the terminal reductant (this work).**

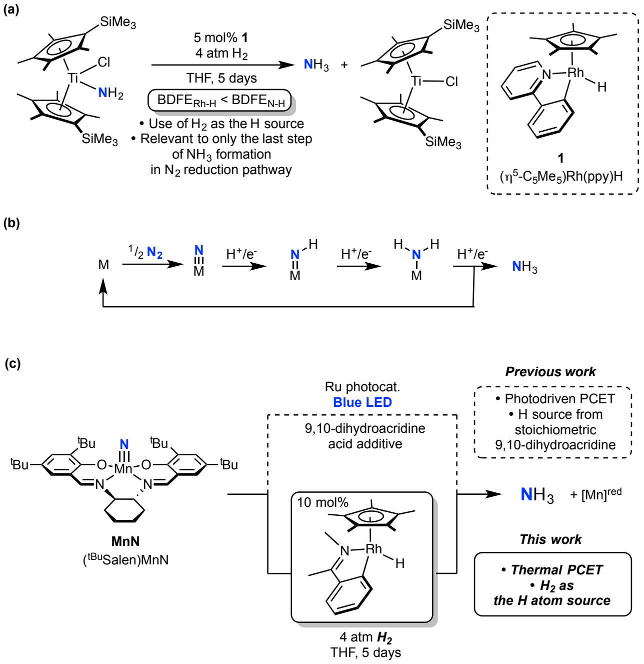

## RESULTS AND DISCUSSION

In exploring the thermal and photostability of **1**, we recently reported its conversion to multimetallic clusters that proved catalytically active for the hydrogenation of *N*-heteroarenes.[35] Because C–H reductive elimination from **1** was identified as the initial step in formation of the multimetallic clusters,[35] modifications to the L–X chelate were explored to improve the stability of the rhodium precatalyst. Initial efforts focused on replacement of the phenylpyridine donor with a phenylimine, owing to the straightforward synthesis and the strong σ-donating character of the imine.[36-39] The *N*-methyl imine derivative, ($\eta^5$-C$_5$Me$_5$)Rh($^{Me}$PhI)H (**2**) ($^{Me}$PhI = *N*-methyl-1-phenylethan-1-imine) was prepared from the chloride precursor, ($\eta^5$-C$_5$Me$_5$)Rh($^{Me}$PhI)Cl and LiHBEt$_3$ (Scheme 2a). The solid-state structures of ($\eta^5$-C$_5$Me$_5$)Rh($^{Me}$PhI)Cl and **2** were determined by X-ray diffraction and the hydride of **2** was located and refined (Scheme 2b, c).

**Scheme 2. (a) Synthesis of 2 with a readily available and modular phenylimine ligand. (b) Solid-state structure of ($\eta^5$-C$_5$Me$_5$)Rh($^{Me}$PhI)Cl as determined by X-ray diffraction. (c) Solid-state structure of 2 determined by X-ray diffraction. All structures at 30% probability ellipsoids with H atoms except for hydride omitted for clarity.**

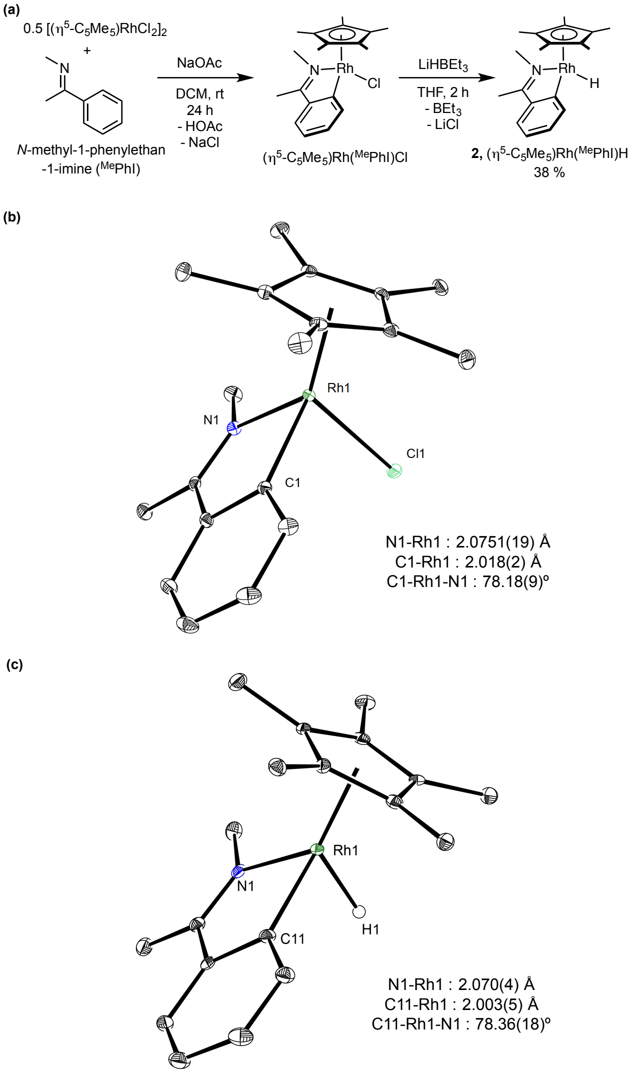

A cyclic imine analogue ($\eta^5$-C$_5$Me$_5$)Rh(4H-ppy)H (**3**) (4H-ppy = 2-phenyl-3,4,5,6-tetrahydropyridine) was isolated in small quantities (6% yield) from exposure of **1** to 4 atm of H$_2$ (Scheme 3a). The majority of the remainder of the material in the hydrogenation was the pentametallic rhodium cluster, ($\eta^5$-C$_5$Me$_5$)$_4$Rh$_5$H$_7$.[35] The solid-state structure of **3** was established by X-ray diffraction (Scheme 3b) and confirmed the partial reduction of the pyridine ring in the phenylpyridine chelate.

**Scheme 3. (a) Synthesis of 3 by partial hydrogenation of the pyridine ring from 1. (b) Solid-state structure of 3 as determined by X-ray diffraction at 30% probability ellipsoids with H atoms except for hydride omitted for clarity.**

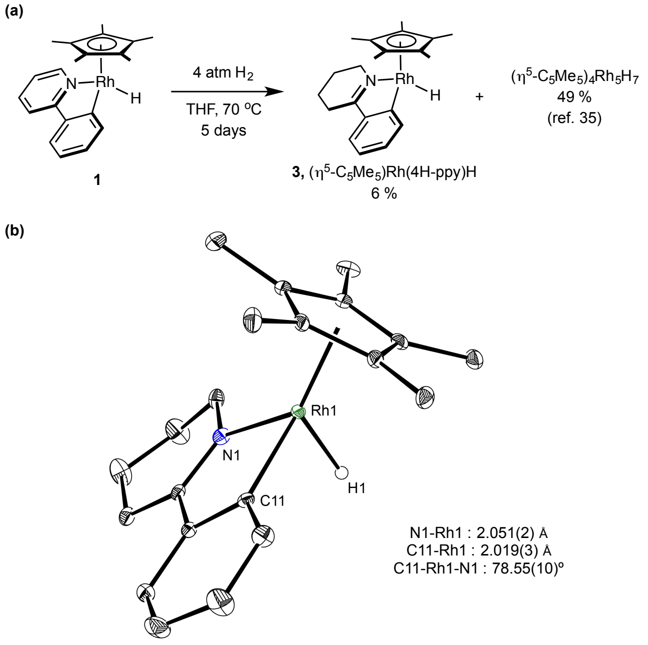

The $^{1}$H NMR chemical shifts of the hydrides and the $^{103}$Rh–H coupling constants in **1**, **2** and **3** support slightly stronger Rh–H bonds in **2** and **3** than **1** (Figure 1). The vibrational frequency of **2** ($\nu_{RhH}$ = 1967 cm$^{-1}$, KBr pellet) by IR spectroscopy is also higher than that of **1** ($\nu_{RhH}$ = 1934 cm$^{-1}$, KBr pellet). However, the DFT computed Rh–H BDFEs of **2** and **3** are 51.8 and 51.5 kcal mol$^{-1}$, respectively, and are indistinguishable from the value of 51.1 kcal mol$^{-1}$ computed for **1**.

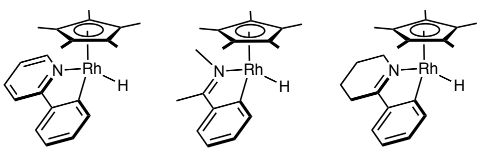

| | **1** | **2** | **3** |
|---|---|---|---|
| **Chemical shift (Rh-*H*, ppm, THF-$d_8$)** | -12.64 | -13.45 | -13.43 |
| **Coupling constant ($^{1}J_{Rh-H}$, Hz, THF-$d_8$)** | 31.6 | 33.1 | 33.2 |
| **Rh-H BDFE (DFT, kcal mol$^{-1}$, gas phase)** | 51.1 | 51.8 | 51.5 |

**Figure 1.** Comparison of the chemical shifts and Rh–H coupling constants of **1**, **2** and **3** from $^{1}$H NMR spectroscopy in THF-$d_8$ and DFT-computed Rh–H BDFEs in gas phase (B3LYP/{6-311+G**,LANL2TZ(-f)}//{6-31G**,LANL2DZ}).

The thermal stability of **2** was evaluated as reductive elimination of phenylpyridine was previously identified as the first step in the formation of the multimetallic clusters from **1** (Scheme 4a).[35] Heating a THF solution of **2** at 60 °C for 24 hours produced no evidence for loss of the *N*-methyl-phenylimine chelate, supporting a higher barrier for C–H reductive elimination (Scheme 4b). The rhodium deuteride, **2-*d*$_1$** was prepared and incorporation of the isotopic label into the phenyl ring was observed after warming a THF-$d_8$ solution of the compound to 50 °C for 24 hours. This observation demonstrates that C(sp$^2$)–H reductive coupling occurs at 50 °C but subsequent ligand dissociation has a higher barrier, likely a result of the relatively strong σ-donation by the imine ligand.

**Scheme 4. (a) Reductive elimination of phenylpyridine from 1. (b) Thermal stability of 2 and deuterium incorporation into the phenyl ring in 2-*d*$_1$.**

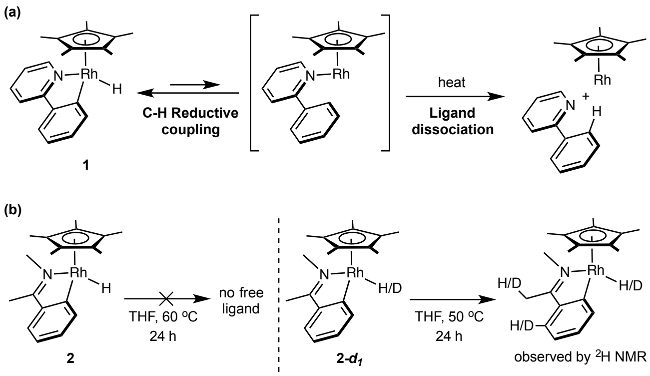

Attempts to determine the Rh–H BDFE in **2** have been unsuccessful. Treatment of a benzene-$d_6$ solution of **2** with 1.05 equivalents of TEMPO, a reagent successfully used for the determination of the BDFE of the Rh–H in **1**,[29] produced several new rhodium products along with TEMPO–H that were detected by $^{1}$H NMR spectroscopy. One of the rhodium products was EPR active with an isotropic signal ($g_{iso}$ = 2.084) consistent with formation of the 17-electron organometallic product (**4**) expected from H-atom transfer (Scheme 5a, b). Upon addition of $H_2$ to this mixture, **2** was cleanly regenerated. Although **4** was present in the solution, a clean and reversible cyclic voltammogram was not obtained due to presence of other rhodium compounds in the mixture. Nevertheless, the p$K_a$ of **2** was determined by titration with TBD (1,5,7-Triazabicyclo[4.4.0]dec-5-ene, p$K_a$ = 21.0 in THF)[40] and a value of 23.2 was measured in THF (Scheme 5c). Deprotonation of **1** by a phosphazene base established a p$K_a$ of 30.3 for **1** in MeCN.[29] Because the p$K_a$ of the phosphazene base in THF is 20.2, the expected p$K_a$ value of **1** in THF is approximately 20.2, lower than that of **2**.

**Scheme 5. (a) Treatment of 2 with 1.05 equivalents TEMPO. (b) X-band EPR spectrum of (a) and the expected paramagnetic product 4. (c) p*K*$_a$ Measurement of 2.**

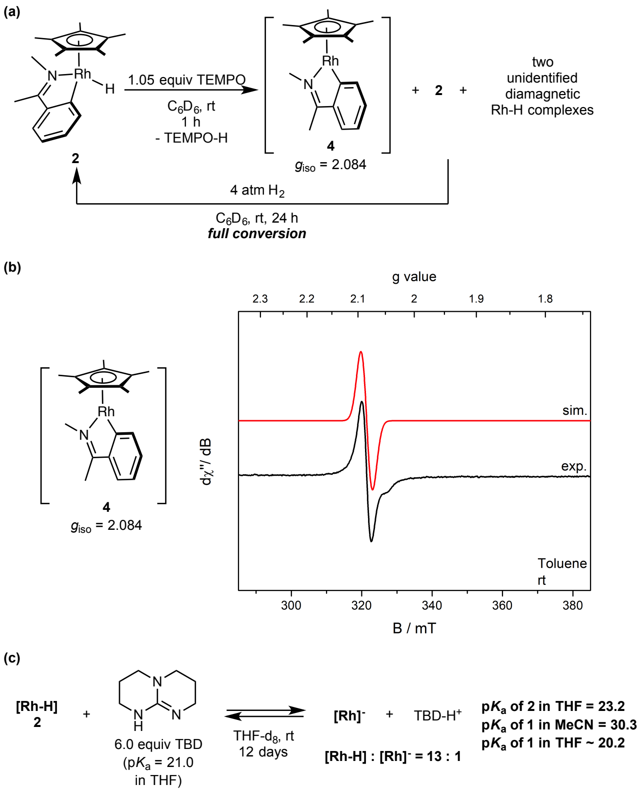

Repeating the experiment with two equivalents of TEMPO resulted in isolation of red crystals and X-ray diffraction established the formation of dimeric rhodium complex, **5** arising from loss of two hydrogen atoms – one from the metal and the other from the imine methyl group (Scheme 6). Identification of this product indicates that the C–H bond of the *α*-methyl imine also has a lower C–H BDFE (62.3 kcal $mol^{-1}$ by DFT computation) than 65 kcal $mol^{-1}$.[41]

**Scheme 6. (a) Formation of 5 from double H-atom abstraction by TEMPO and DFT-computed C–H BDFE in gas phase (B3LYP/{6-311+G**,LANL2TZ(-f)}//{6-31G**,LANL2DZ}). (b) Solid-state structure of 5 at 30% probability ellipsoids with H atoms omitted for clarity.**

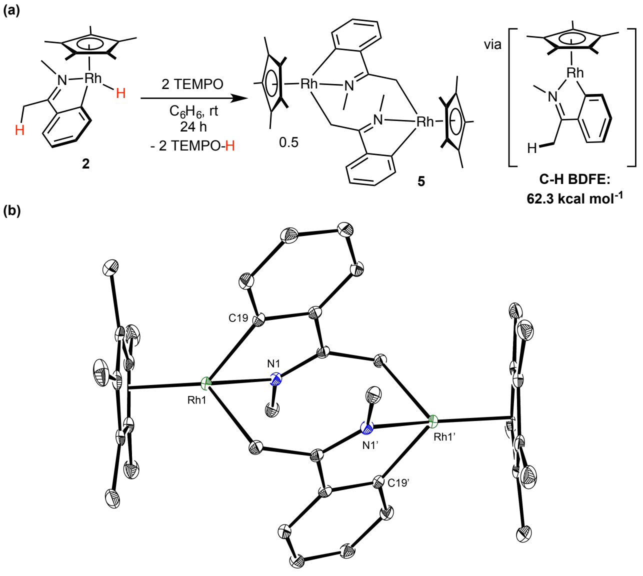

With a new rhodium hydride in hand, the catalytic performance of **2** for the hydrogenation of **MnN** was examined (Table 1). With 5 mol% of **2** under 4 atm of $H_2$ in THF, 22% of $NH_3$ was obtained after 5 days at 23 °C (Table 1, entry 1). Notably, **1** did not yield any $NH_3$ under the same conditions (entry 2). The cyclic imine derivative, **3** produced $NH_3$ in 21% yield almost identical to the results with **2** (entry 3). Previous studies have established that addition of L-type ligands to ammonia synthesis reactions with **MnN** increases the yield of free $NH_3$, likely by outcompeting ammonia coordination to the manganese.[25,26] Repeating the hydrogenation of **MnN** with 10 mol% of **2** at higher concentration and addition of two equivalents of TMEDA (*N,N,N′,N′*-tetramethylethylenediamine) increased the yield of $NH_3$ to 40% (entry 4). Again, **1** produced no $NH_3$ under these conditions (entry 5). Increasing the temperature of the hydrogenation to 50 °C improved the performance of **2** and yielded 60% yield free $NH_3$ after 5 days (entry 6). Although the total turnovers based on the amount of free $NH_3$ are only 6.0, turnovers by the number of PCET event (H·) are 18, comparable to the 19 turnovers reported for catalytic $NH_3$ formation from the titanocene amide with **1** after 5 days.[20,21] In the absence of a rhodium complex, no $NH_3$ was generated and demonstrating that TMEDA is not the source of the hydrogen atom (entry 7).

**Table 1. Evaluation of catalytic MnN hydrogenation to free $NH_3$ with 1, 2 and 3.**

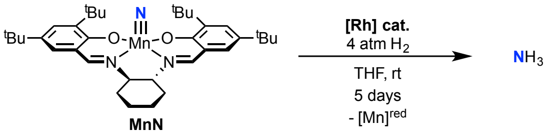

| entry | conditions | $NH_3$ yield (%)[a] | TON ($NH_3$) | TON (H·) |
|---|---|---|---|---|
| 1[b] | 5 mol% **2** | 22 | 4.4 | 13 |
| 2[b] | 5 mol% **1** | < 1 | - | - |
| 3[b] | 5 mol% **3** | 21 | 4.2 | 13 |
| 4[c] | 10 mol% **2**, 2 equiv TMEDA | 40 | 4.0 | 12 |
| 5[c] | 10 mol% **1**, 2 equiv TMEDA | < 1 | - | - |
| 6[c] | 10 mol% **2**, 2 equiv TMEDA, 50 °C | 60 | 6.0 | 18 |
| 7[c] | no Rh catalyst, 2 equiv TMEDA | <1 | - | - |

[a]The volatiles were vacuum transferred on to an HCl solution in $Et_2O$ and the yield of $NH_4Cl$ was determined by $^1H$ NMR spectroscopy using 1,2-dichloroethane as an internal standard. [b]0.20 M concentration. [c]0.40 M concentration.

To confirm the **MnN** as the source of ammonia, the $^{15}N$-labeled isotopologue, **$Mn^{15}N$** was prepared (Scheme 7a). Under the hydrogenation conditions at room temperature (Table 1, entry 4), 31% of $^{15}NH_3$ was obtained as judged by $^1H$ NMR spectroscopy. Treatment of the non-volatile product with $C_2Cl_6$ produced the manganese chloride ($^{tBu}$Salen)MnCl as confirmed by comparison of the UV-Vis spectrum to an authentic sample (Scheme 7b). This result also demonstrates that the salen ligand remains intact under the hydrogenation conditions with **2**. The starting nitride **MnN** was regenerated in 40% yield by treatment with aqueous $NH_3$ followed by bleach (Scheme 7b).

**Scheme 7. (a) Catalytic hydrogenation of ($^{tBu}$Salen)Mn≡$^{15}$N (Mn$^{15}$N) to $^{15}NH_3$. (b) Chlorination and oxidation of the non-volatile residue to regenerate MnN.**

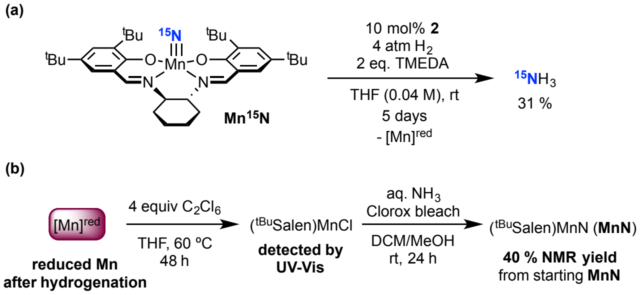

The difference between the hydrogenation performance of **1** and **2** is remarkable given their comparable BDFEs. To gain additional insight, stoichiometric experiments were conducted whereby two equivalents **MnN** were treated with one equivalent of either **1** or **2** (Scheme 8). With **2** the successful hydrogenation of the precatalyst was supported by disappearance of the $^1$H NMR resonances of both metal complexes and observation of a strong isotropic signal ($g_{iso}$ = 2.046) by EPR spectroscopy at 23 °C, presumably corresponding to the reduced [(Salen)Mn] (Scheme 8a).[25] In addition, the metal nitride stretch ($\nu_{MnN}$ = 1049 $cm^{-1}$, KBr pellet)[42] was not observed in the infrared spectrum. The signal of Rh–H also disappeared in both the $^1$H NMR and IR spectra. It is likely that H-atom transfer from the rhodium to the nitride occurs, resulting in the disappearance of the manganese nitride stretch in the IR spectrum. Addition of 4 atm $H_2$ to this product regenerated **2** over the course of 48 hours as confirmed by $^1$H NMR spectroscopy. In these experiments, there was no spectroscopic evidence for the formation of detectable quantities of **5**.

**Scheme 8. Stoichiometric reactions of MnN with (a) 2 and (b) 1 in THF and (c) stacked X-band spectra measured at 0.02 M concentration.**

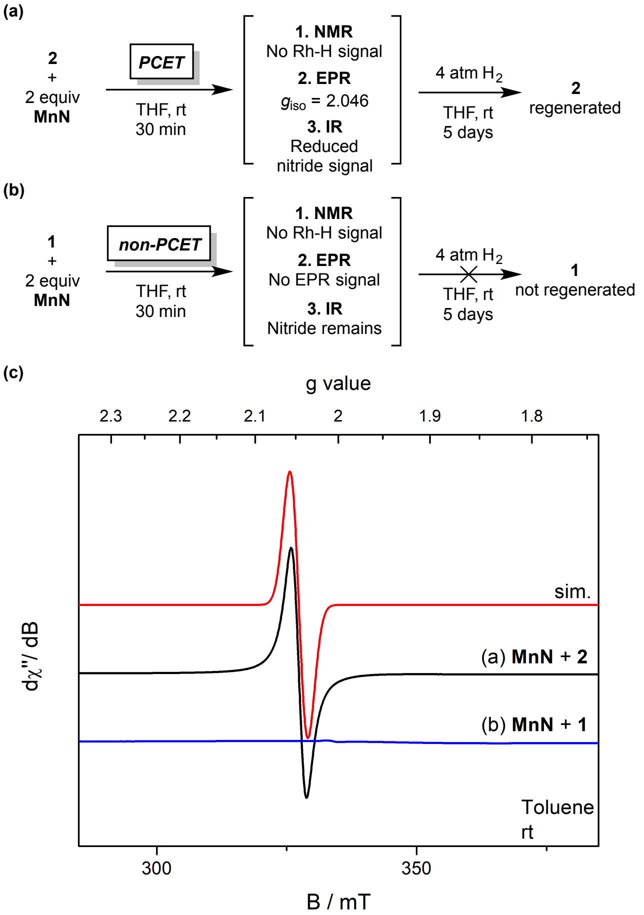

In contrast, addition of **1** to two equivalents **MnN** generated a red-colored solution within 30 min and analysis by $^1$H NMR spectroscopy established disappearance of the resonances of the metal complexes including the Rh–H signal (Scheme 8b). Importantly, no signal was observed by EPR spectroscopy and the nitride signal remained in the IR spectrum. Addition of 4 atm $H_2$ to the mixture did not regenerate **1**, establishing deactivation of the rhodium from interaction with **MnN**.

The above deactivation process suggests that the Rh–H in **1** reacts by a pathway other than PCET such as proton or hydride transfer (Scheme 9). Addition of **1** to two equivalents **MnN** in acetonitrile yielded the cationic rhodium acetonitrile derivative, $[(\eta^5\text{-}C_5Me_5)Rh(ppy)(MeCN)]^+$ (**6**),[28] which was detected by IR spectroscopy, ruling out the possibility of proton transfer. It was previously reported that the cationic **6** was unreactive with $H_2$ to regenerate **1** in the absence of an appropriate base.[29] Because the nitride signal remained in the IR spectrum, it is likely that the hydride was transferred into the electrophilic imine backbone of the salen ligand to produce an anionic manganese(V) complex.[43-46] On the other hand, the reaction of **2** and **MnN** did not yield the cationic species, $[(\eta^5\text{-}C_5Me_5)Rh(^{Me}PhI)(MeCN)]^+$, which was independently prepared and structurally characterized (SI S6, Figure S12-S14).

**Scheme 9. Stoichiometric reaction between MnN and 1 in acetonitrile to yield 6.**

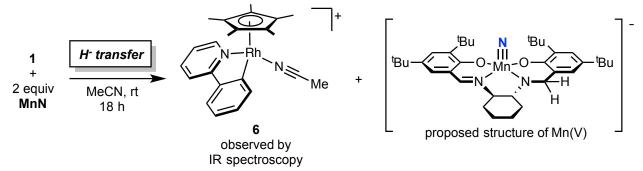

To suppress the formation of **6**, hydrogenation in a non-polar, non-coordinating solvent was explored. The stoichiometric reaction of **1** and two equivalents **MnN** in benzene produced an isotropic EPR signal identical to the signal observed from mixing **MnN** and **2** in THF (Scheme 10a). Under catalytic conditions, 25% free ammonia was observed with 10 mol% **1** for 5 days at 23 °C in benzene (Scheme 10b). Although the number of catalytic turnovers (2.5 for $NH_3$, 7.5 for H·) is modest, these results demonstrate that solvent selection can be used to suppress deleterious hydride transfer pathways.

**Scheme 10. (a) Stoichiometric reaction between MnN and 1 in benzene. (b) Catalytic hydrogenation of MnN using 1 as the precatalyst in benzene.**

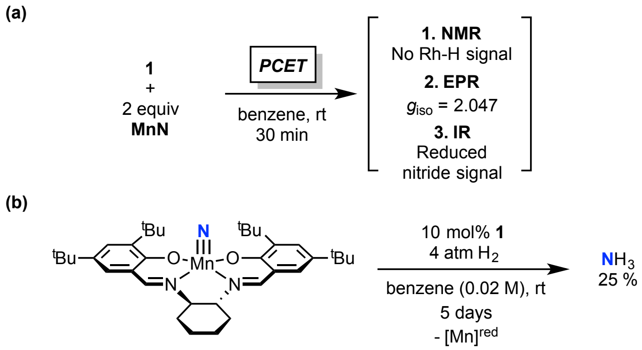

## CONCLUSIONS

In conclusion, a rare hydrogenation of a metal nitride using well-defined rhodium $H_2$ activation and hydrogen atom transfer precatalysts is described. Although the bond dissociation free energies are indistinguishable, the phenylimine ($^{Me}$PhI) variant of the rhodium precatalyst was more efficient due to the propensity to promote PCET over competing, deleterious hydride transfer pathways. With the phenylpyridine (ppy) variant, this side reaction was suppressed by use of non-polar, non-coordinating solvents. These findings provide important fundamental understanding and ultimately design principles for $H_2$ activation and proton coupled electron transfer catalysts for catalytic ammonia synthesis as well as other potential applications.

## ASSOCIATED CONTENT

### Supporting Information

The Supporting Information is available free of charge on the ACS Publications website.

General considerations; preparation of transition metal complexes; general procedures; spectroscopic and crystallographic data
Crystallographic data for ($\eta^5$-$C_5Me_5$)Rh($^{Me}$PhI)Cl
Crystallographic data for **2**
Crystallographic data for **3**
Crystallographic data for **5**
Crystallographic data for [($\eta^5$-$C_5Me_5$)Rh(MePhI)(MeCN)][$BArF_{24}$]

## AUTHOR INFORMATION

### Corresponding Author

*pchirik@princeton.edu

### ORCID

Sangmin Kim: 0000-0002-7289-0693
Hongyu Zhong: 0000-0002-6892-482X
Yoonsu Park: 0000-0003-1511-0635
Florian Loose: 0000-0003-1643-4607
Paul J. Chirik: 0000-0001-8473-2898

### Notes

The authors declare no competing financial interest.

## ACKNOWLEDGMENT

This research was supported by the U.S. Department of Energy, Office of Science, Office of Basic Energy Sciences, Catalysis Science program, under Award DE-SC0006498. S.K. acknowledges Samsung Scholarship for financial support.

## REFERENCES

(1) MacKay, B. A.; Fryzuk, M. D. Dinitrogen Coordination Chemistry: On the Biomimetic Borderlands. *Chem. Rev.* **2004**, *104*, 385-402.

(2) Gambarotta, S. Dinitrogen Fixation and Activation After 30 Years: A Puzzle Still Unsolved. *J. Organomet. Chem.* **1995**, *500*, 117-126.

(3) Hager, T. in *The Alchemy of Air*, Three River Press, New York, **2008**.

(4) Smil, V. in *Enriching the Earth: Fritz Haber, Carl Bosch, and the Transformation of World Food Production*, MIT Press, Cambridge, MA, **2004**.

(5) Haber, F.; van Oordt, G. Über die Bildung von Ammoniak aus den Elementen. *Z. Anorg. Chem.* **1905**, *47*, 42-44.

(6) Topham, S. A. in *The History of the Catalytic Synthesis of Ammonia BT - Catalysis: Science and Technology* (Eds.: Anderson, J.R.; Boudart, M), Springer, Berlin, Heidelberg, 1985, pp. 1-50.

(7) Yandulov, D. V.; Schrock, R. R. Catalytic Reduction of Dinitrogen to Ammonia at a Single Molybdenum Center. *Science* **2003**, *301*, 76-78.

(8) Eizawa, A.; Nishibayashi, Y. Catalytic Nitrogen Fixation Using Molybdenum-Dinitrogen Complexes as Catalysts. *Top. Organomet. Chem.* **2017**, *60*, 153-170.

(9) Tanaka, H.; Yoshizawa, K. Computational Approach to Nitrogen Fixation on Molybdenum-Dinitrogen Complexes. *Top. Organomet. Chem.* **2017**, *60*, 171-196.

(10) Kuriyama, S.; Nishibayashi, Y. Catalytic Transformations of Molecular Dinitrogen by Iron and Cobalt-Dinitrogen Complexes as Catalysts. *Top. Organomet. Chem.* **2017**, *60*, 215-234.

(11) Tanaka, H.; Nishibayashi, Y.; Yoshizawa, K. Interplay between Theory and Experiment for Ammonia Synthesis Catalyzed by Transition Metal Complexes. *Acc. Chem. Res.* **2016**, *49*, 987-995.

(12) Nishibayashi, Y. Recent Progress in Transition-Metal-Catalyzed Reduction of Molecular Dinitrogen under Ambient Reaction Conditions. *Inorg. Chem.* **2015**, *54*, 9234-9247.

(13) MacLeod, K. C.; Holland, P. L. Recent Developments in the Homogeneous Reduction of Dinitrogen by Molybdenum and Iron. *Nat Chem.* **2013**, *5*, 559-565.

(14) Arashiba, K.; Miyake, Y.; Nishibayashi, Y. A Molybdenum Complex Bearing PNP-type Pincer Ligands Leads to the Catalytic Reduction of Dinitrogen into Ammonia. *Nat. Chem.* **2011**, *3*, 120-125.

(15) Tanaka, H.; Arashiba, K.; Kuriyama, S.; Sasada, A.; Nakajima, K.; Yoshizawa, K.; Nishibayashi, Y. Unique Behaviour of Dinitrogen-Bridged

Dimolybdenum Complexes Bearing Pincer Ligand Towards Catalytic Formation of Ammonia. *Nat. Commun.* **2014**, *5*, 3737.

(16) Kuriyama, S.; Arashiba, K.; Nakajima, K.; Matsuo, Y.; Tanaka, H.; Ishii, K.; Yoshizawa, K.; Nishibayashi, Y. Catalytic Transformation of Dinitrogen into Ammonia and Hydrazine by Iron-Dinitrogen Complexes Bearing Pincer Ligand. *Nat. Commun.* **2016**, *7*, 12181.

(17) Eizawa, A.; Arashiba, K.; Tanaka, H.; Kuriyama, S.; Matsuo, Y.; Nakajima, K.; Yoshizawa, K.; Nishibayashi, Y. Remarkable Catalytic Activity of Dinitrogen-Bridged Dimolybdenum Complexes Bearing NHC-Based PCP-Pincer Ligands Toward Nitrogen Fixation. *Nat. Commun.* **2017**, *8*. 14874.

(18) Anderson, J. S.; Rittle, J.; Peters, J. C. Catalytic Conversion of Nitrogen to Ammonia by an Iron Model Complex. *Nature* **2013**, *501*, 84-87.

(19) Bezdek, M. J.; Pappas, I.; Chirik, P. J. Determining and Understanding N–H Bond Strengths in Synthetic Nitrogen Fixation Cycles. *Top. Organomet. Chem.* **2017**, *60*, 1-22.

(20) Pappas, I.; Chirik, P. J. Ammonia Synthesis by Hydrogenolysis of Titanium-Nitrogen Bonds Using Proton Coupled Electron Transfer. *J. Am. Chem. Soc.* **2015**, *137*, 3498-3501.

(21) Pappas, I.; Chirik, P. J. Catalytic Proton Coupled Electron Transfer from Metal Hydrides to Titanocene Amides, Hydrazines and Imides: Determination of Thermodynamic Parameters Relevant to Nitrogen Fixation. *J. Am. Chem. Soc.* **2016**, *138*, 13379-13389.

(22) Bezdek, M. J.; Chirik, P. J. A Fresh Approach to Synthesizing Ammonia from Air and Water. *Nature* **2019**, *568*, 464-466.

(23) Ashida, Y.; Arashiba, K.; Nakajima, K.; Nishibayashi, Y. Molybdenum-Catalysed Ammonia Production with Samarium Diiodide and Alcohols or Water. *Nature* **2019**, *568*, 536-540.

(24) Bruch, Q. J.; Connor, G. P.; Chen, C.; Holland, P. L.; Mayer, J. M.; Hasanayn, F.; Miller, A. J. M. Dinitrogen Reduction to Ammonia at Rhenium Utilizing Light and Proton-Coupled Electron Transfer. *J. Am. Chem. Soc.* **2019**, *141*, 20198-20208.

(25) Wang, D.; Loose, F.; Chirik, P. J.; Knowles, R. R. N–H Bond Formation in a Manganese(V) Nitride Yields Ammonia by Light-Driven Proton-Coupled Electron Transfer. *J. Am. Chem. Soc.* **2019**, *141*, 4795-4799.

(26) Loose, F.; Wang, D.; Tian, L.; Scholes, G. D.; Knowles, R. R.; Chirik, P. J. Evaluation of Excited State Bond Weakening for Ammonia Synthesis from a Manganese Nitride: Stepwise Proton Coupled Electron Transfer is Preferred over Hydrogen Atom Transfer. *Chem. Commun.* **2019**, *55*, 5595-5598.

(27) Scepaniak, J. J.; Young, J. A.; Bontchev, R. P.; Smith, J. M. Formation of Ammonia from an Iron Nitrido Complex. *Angew. Chem., Int. Ed.* **2009**, *48*, 3158-3160.

(28) Hu, Y.; Li, L.; Shaw, A. P.; Norton, J. R.; Sattler, W.; Rong, Y. Synthesis, Electrochemistry, and Reactivity of New Iridium(III) and Rhodium(III) Hydrides. *Organometallics* **2012**, *31*, 5058-5064.

(29) Hu, Y.; Norton, J. R. Kinetics and Thermodynamics of $H^-/H\cdot/H^+$ Transfer from a Rhodium(III) Hydride. *J. Am. Chem. Soc.* **2014**, *136*, 5938-5948.

(30) Bezdek, M. J.; Chirik, P. J. Pyridine(diimine) Chelate Hydrogenation in a Molybdenum Nitrido Ethylene Complex. *Organometallics* **2019**, *38*, 1682-1687.

(31) Rebreyend, C.; de Bruin, B. Photolytic $N_2$ Splitting: A Road to Sustainable $NH_3$ Production? *Angew. Chem., Int. Ed.* **2015**, *54*, 42-44.

(32) Klopsch, I.; Yuzik-Klimova, E. Y.; Schneider, S. Functionalization of $N_2$ by Mid to Late Transition Metals via N–N Bond Cleavage. *Top. Organomet. Chem.* **2017**, *60*, 71-112.

(33) Klopsch, I.; Kinauer, M.; Finger, M.; Würtele, C.; Schneider, S. Conversion of Dinitrogen into Acetonitrile under Ambient Conditions. *Angew. Chem., Int. Ed.* **2016**, *55*, 4786-4789.

(34) Bezdek, M. J.; Chirik, P. J. Expanding Boundaries: $N_2$ Cleavage and Functionalization Beyond Early Transition Metals. *Angew. Chem., Int. Ed.* **2016**, *55*, 7892-7896.

(35) Kim, S.; Loose, F.; Bezdek, M. J.; Wang, X.; Chirik, P. J. Hydrogenation of *N*-Heteroarenes Using Rhodium Precatalysts: Reductive Elimination Leads to Formation of Multimetallic Clusters. *J. Am. Chem. Soc.* **2019**, *141*, 17900-17908.

(36) Conifer, C. M.; Law, D. J.; Sunley, G. J.; Haynes, A.; Wells, J. R.; White, A. J. P.; Britovsek, G. J. P. Dicarbonylrhodium(I) Complexes of Bipyridine Ligands with Proximate H–Bonding Substituents and Their Application in Methyl Acetate Carbonylation. *Eur. J. Inorg. Chem.* **2011**, 3511-3522.

(37) Poel, H. V. D.; Koten, G. V.; Vrieze, K. Four-co-ordinate Rhodium(I) Complexes $[\{Rh(CO)_2Cl\}_n(\alpha\text{-diimine})]$ (n = 1, 2) with σ,σ-N,N' Chelate or σ-N, σ-N' Bridge Bonded RN=C(R')C(R")=NR Lgands. Influence of the Branching at $C^\alpha$ of R on the $Rh^I$–α-diimine Interaction. *Inorg. Chim. Acta* **1981**, *51*, 253-262.

(38) Delgado-Laita, E.; Sanchez-Muñoyerro, E. Carbonyl Rhodium(I) Complexes with α-Diimines Ligands. *Polyhedron* **1984**, *3*, 799-804.

(39) Simões, J. A. M.; Beauchamp, J. L. Transition Metal-Hydrogen and Metal-Carbon Bond Strengths: The Keys to Catalysis. *Chem. Rev.* **1990**, *90*, 629-688.

(40) Tshepelevitsh, S.; Kütt, A.; Lõkov, M.; Kaljurand, I.; Saame, J.; Heering, A.; Plieger, P. G.; Vianello, R.; Leito, I. On the Basicity of Organic Bases in Different Media. *Eur. J. Org. Chem.* **2019**, 6735-6748.

(41) Warren, J. J.; Tronic, T. A.; Mayer, J. M. Thermochemistry of Proton-Coupled Electron Transfer Reagents and its Implications. *Chem. Rev.* **2010**, *110*, 6961-7001.

(42) Clarke, R. M.; Storr, T. Tuning Electronic Structure to Control Manganese Nitride Activation. *J. Am. Chem. Soc.* **2016**, *138*, 15299-15302.

(43) Chiu, S.-M.; Wong, T.-W.; Man, W.-L.; Wong, W.-T.; Peng, S.-M.; Lau, T.-C. Facile Nucleophilic Addition to Salophen Coordinated to Nitridoosmium(VI). *J. Am. Chem. Soc.* **2001**, *123*, 12720-12721.

(44) Matsumoto, K.; Sawada, Y.; Saito, B.; Sakai, K.; Katsuki, T. Construction of Pseudo-Heterochiral and Homochiral Di-μ-oxotitanium(Schiff base) Dimers and Enantioselective Epoxidation Using Aqueous Hydrogen Peroxide. *Angew. Chem., Int. Ed.* **2005**, *44*, 4935-4939.

(45) Ziegler, J. E.; Du, G.; Fanwick, P. E.; Abu-Omar, M. M. An Efficient Method for the Preparation of Oxo Molybdenum Salalen Complexes and Their Unusual Use as Hydrosilylation Catalysts. *Inorg. Chem.* **2009**, *48*, 11290-11296.

(46) Ji, J.; Chen, X.; Wang, C.-J.; Jia, A.-Q.; Zhang, Q.-F. Syntheses, Structures and Electrochemical Properties of Ruthenium(II/III) Complexes with Tetradentate Schiff Base Ligands. *J. Coord. Chem.* **2019**, *72*, 480-490.

# For Table of Contents Use